SEMARAK ILMU PUBLISHING

Journal of Advanced Research in Applied Sciences and Engineering Technology

Journal homepage:
https://semarakilmu.com.my/journals/index.php/applied_sciences_eng_tech/index
ISSN: 2462-1943

A Robust Deep Learning Model for Brain Tumor Detection and Classification Using Efficient Net: A Brief Meta-Analysis

Retinderdeep Singh[1], Chander Prabha[1,*], Meena Malik[2], Ankur Goyal[3]

[1] Chitkara University Institute of Engineering and Technology, Chitkara University, Punjab, India
[2] Chandigarh University, Mohali, Punjab, India
[3] Symbiosis Institute of Technology, Symbiosis International Deemed University, Pune Maharashtra, India

ARTICLE INFO

Article history:
Received
Received in revised form
Accepted
Available online

Keywords:

Brain tumor detection; EfficientNet; deep learning; model performance; Softmax activation; ReLU activation; Adam optimizer

ABSTRACT

Accurately detecting and classifying brain tumors', is critical for timely diagnosis and effective treatment planning. The purpose of this paper is to provide a comprehensive examination utilizing the EfficientNet family of deep learning architectures to automatically identify and categorize three forms of brain tumors from magnetic resonance imaging (MRI) scans. The primary aim of the study is to assess the performance of different EfficientNet models (ranging from EfficientNet-B0 to EfficientNet-B7) and determine their capability to achieve high accuracy in brain tumor classification. In the implementation, a diverse dataset is compiled comprising approximately 18,500 MRI images, representing various types of brain tumors. EfficientNet models are trained, validated, and tested using a combination of Softmax and ReLU activation functions, along with the Adam optimizer by employing learning rates of 0.0005 and 0.00001 for model training and optimization. The experimental results underscore the significant potential of the EfficientNet family in brain tumor classification. The findings reveal a consistent improvement in tumor detection accuracy as model complexity increases. The attained accuracies for different EfficientNet models are; 96.07% (EfficientNet-B0), 97.86% (EfficientNet-B1), 98.21% (EfficientNet-B2), 97.86% (EfficientNet-B3), 98.93% (EfficientNet-B4), 99.64% (EfficientNet-B5), 98.57% (EfficientNet-B6), and 99.64% (EfficientNet-B7), respectively. The proposed research not only validates the efficiency of the EfficientNet architecture in classifying brain tumors but also offers valuable insights into how model complexity influences classification performance. The notably high accuracy rates emphasize the clinical promise of employing deep learning methods to aid radiologists and medical experts in precise and efficient brain tumor diagnosis. Additionally, the paper's scope adds to the growing body of knowledge regarding the application of deep learning techniques to enhance medical image analysis and diagnostic capabilities.

1. Introduction

The human brain, often hailed as the most intricate and awe-inspiring organ within the human body, stands as a marvel of biological engineering. With a weight of approximately three pounds

* *Corresponding author.*
E-mail address: prabhanice@gmail.com

https://doi.org/10.37934/araset.49.2.2651

(about 1.4 kilograms) and composed of countless neurons, it functions as the central hub of human cognition, emotions, and consciousness. This intricate organ not only oversees essential bodily functions like breathing and heart rate but also facilitates processes such as thinking, learning, memory, and a diverse array of emotions. Its elaborate network of neural connections enables the interpretation and processing of sensory inputs from the external world, enabling us to perceive, comprehend, and interact with our surroundings. Furthermore, the brain's remarkable adaptability and plasticity empower it to learn, reorganize, and recuperate after injury, underscoring the human potential for development, creativity, and resilience. The quest to unravel the enigmas of the human brain remains an absorbing expedition for scientists and researchers, as it holds the promise of unveiling the intricacies of human behavior and the essence of consciousness itself [1].

1.1 Brain Tumor

A brain tumor (BT) refers to the abnormal growth of brain cells or their neighbouring structures. These growths can be categorized as either non-cancerous (benign) or cancerous (malignant) and can originate from various types of brain tissue, including glial cells, neurons, and the brain's protective membranes (meninges). BTs have the potential to disrupt normal brain functions, impacting cognitive abilities, motor skills, and sensory perception. Symptoms may vary based on reasons such as the tumor’s size, location, and rate of growth, but common indications include headaches, seizures, alterations in vision or speech, and neurological impairments. Early detection and treatment are vital, as some BTs can be life-threatening if left untreated. Treatment options typically encompass radiation therapy, surgery, chemotherapy, or all of these methods, tailored to the specific tumor type and characteristics. Ongoing research into the causes and treatments of BTs aims to enhance the prognosis and quality of life for individuals grappling with these complex medical conditions [2]. This study mainly focuses on classifying three types of BT, glioma tumor (GT), meningioma tumor (MT), and pituitary tumor (PT).

1.1.1 Glioma tumor

The GTs are primary BTs that develop from cells called glial, which are supportive cells found in the central nervous system. These tumors can manifest in diverse regions of the brain and spinal cord and are classified according to both their cell of origin and their degree of malignancy [3]. The effective treatment of this tumor is primarily possible when it is detected in its early stages. Globally, primary central nervous system (CNS) and BTs were responsible for an estimated 251,329 deaths in 2020 [4]. According to data from the IARC (International Association of Cancer Registries), India records approximately 28,000 cases of BTs annually, and tragically, 24,000 individuals lose their lives to BTs [5].

1.1.2 Meningioma tumor

The MT is a type of BT that originates in the meninges, the protective tissues surrounding the brain. Generally, MTs are typically non-cancerous, although in rare cases, they can become malignant. These tumors are most commonly found on the top and outer surface of the brain, and occasionally, they can develop at the base of the skull. Spinal MTs are relatively uncommon. The incidence of MT is approximately 97 cases per 100,000 individuals [6]. There are currently three grades of MTs.

i. Typical or Grade I MT- These tumors grow slowly and account for approximately 80% of cases.
ii. Grade II or atypical MT- These tumors have a faster growth rate and can be more challenging to treat. They represent about 17% of cases.
iii. Malignant (cancerous) MT of Grade III- Also known as anaplastic MT, these tumors grow and spread rapidly and are seen in a little over 1.7% of cases.

1.1.3 Pituitary tumor

Medically known as a pituitary adenoma, is an abnormal growth of cells in the pituitary gland, A minute, pea-sized gland located at the base of the brain. The pituitary gland plays a pivotal role in regulating various bodily functions by producing hormones responsible for controlling growth, metabolism, reproduction, and responses to stress, among other functions. PTs can be benign (non-cancerous) or, in rare instances, malignant (cancerous). Depending on their size and location within the pituitary gland, these tumors can disrupt the normal production and release of hormones, leading to a wide array of symptoms. Common signs include hormonal imbalances, vision issues, headaches, and, in some cases, alterations in behavior. Treatment options for PTs may include radiation therapy, medication, surgical removal, or a combination of these methods. Timely diagnosis and appropriate management are essential to minimize potential complications and enhance the quality of life for individuals dealing with PTs [7].

It is very important to detect tumors in the early stages so that there are fewer complexities in the treatment, the tumor is generally detected using MRI scans. In this study, EfficientNet family models are comparatively analyzed to check the highest accuracy in detecting and classifying types of BT using MRI scans. The models are trained to detect BT using a publicly available dataset containing approximately 18500 images of MRI scans. After training, the models take MRI scans as input and detect the type of tumor as depicted in Figure 1.

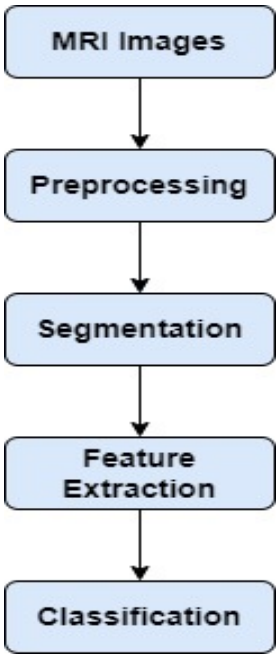

Fig. 1. BT detection system

1.2 Problem Statement

Early diagnosis of brain tumors is essential for enhancing therapeutic results, protecting brain function, lowering healthcare expenditures, and enhancing the general health and survival rates of afflicted people. Early detection of brain tumors is of paramount importance due to its significant impact on patient outcomes and treatment options. Here are several reasons highlighting the importance of early detection: Improved Survival Rates, Optimal Treatment Planning, Preservation of Brain Function, Reduced Treatment Complexity, Lower Healthcare Costs, Prevention of Complications, Enhanced Quality of Life, Clinical Trials and Research, Psychological Well-being, Long-Term Monitoring

1.3 Objective

The primary objective of this research study is to showcase the capabilities of sophisticated deep learning algorithms, namely the EfficientNet family, in accurately and efficiently classifying brain tumors. The final aim is to make a valuable contribution to the field of medical picture analysis and enhance diagnostic capacities in this domain.

1.4 Contribution of the Paper

The significance of this article lies in its capacity to contribute to the advancement of brain tumor identification, improvement of patient care, and provision of valuable insights and practical resources for scholars and medical practitioners engaged in the field of neurodegenerative diseases. Some of the notable contributions include Significant Contribution to the Discipline: The article's findings about the high accuracy rates in identifying brain tumor illness contribute significantly to the field. The attainment of an accurate diagnosis has significant importance in improving patient outcomes, especially during the first phases of the disease. The present study examines innovative methodologies for enhancing pre-existing models in the context of medical image analysis, with a specific emphasis on the identification of brain tumor diseases. In performance evaluation, this study comprehensively evaluates the performance of several EfficientNet models (ranging from B0 to B7) in the classification of BT. This involves assessing the precision, recall, accuracy, and F1-score to get a comprehensive understanding of the model's capabilities.

1.4.1 Further the paper's structure

i. Section 2 - The article proposes a unique technique for identifying BTs used in the research under the proposed methodology part.
ii. Section 3 – Results section presents and discusses the results obtained from the proposed model's application.
iii. Section 4 - Summarizes the findings and suggests potential avenues for future research.

1.5 Literature Review

This section provides an extensive review of prior research in the field of tumor detection using Deep Learning (DL) as shown in Table 1. A brief summary of pertinent literature on tumor identification is provided in this section. It examines past research projects and contrasts the results

of such efforts. Additionally, it includes a comparative analysis from the previous studies [8-17], offering insights into the state of the art in tumor detection utilizing DL techniques.

Table 1
Summary of work done by researchers

Author	Description/Review	Year	Model	Results
Mishra *et al.,* [8]	Outlined an efficient deep learning technique for BT classification known as inductive transfer learning. It used both 3D and 2D datasets to extract intricate characteristics from brain MRI data using the EfficientNet model. The model's outstanding accuracy of 98.78% allowed it to classify BTs into four different categories.	2022	EfficientNet	98.78%
Mahesh *et al.,* [9]	The Contour Extraction Extended EfficientNet-B0 (CE-EEN-B0), a deep Convolutional Neural Network (CNN), model is suggested as a way to identify BTs depending on where in the brain they are located. BTs are divided into four groups under this model: no tumor, PT, MT, and GT. It outperformed current pre-trained networks with a high accuracy score of 97.24%.	2023	EfficientNet-B0	97.24%
Isunuri and Kakarla [10]	BT grade categorization using a method integrating the EfficientNet model, multi-path convolution, and multi-head attention network. A pre-trained EfficientNetB4 is used to extract the features, and then multi-path convolution and attention are used to improve the features. The dataset from TCIA consists of normal, low-grade, and high-grade instances. The model's accuracy is a remarkable 98.35%.	2023	EfficientNet-B4	98.35%
Goutham *et al.,* [11]	A system that can detect GT, MT, and PT using a GUI application. EfficientNet-B0 model is used to classify these types of tumors. The model was trained using MRI scans and can detect BT within minutes. The system achieved an accuracy of 96.94%.	2022	EfficientNet-B0	96.94%
Mantha and Reddy [12]	The suggested method used the EfficientNet-B3 deep learning model to create an automated approach for categorizing BT kinds from MRI data. Three different forms of BT, GT, MT, and PT may be detected by the system. The model's excellent accuracy of 99.35% was attained. The classification results show 99% accuracy for precision, recall, and f1-score.	2021	EfficientNet-B3	99.35%
Zulfiqar *et al.,* [13]	Compared five fine-tuned EfficientNet models (EfficientNet-B0 - EfficientNet-B4) and created a system to classify BT types into 3 categories (GT, MT, and PT). The models were trained using a publicly available CE-MRI dataset. Data augmentation's impact on test accuracy was studied, and Grad-CAM visualization highlights tumor regions. The best-performing model, using EfficientNetB2, achieved a high overall test accuracy (98.86%), precision (98.65%), recall (98.77%), and F1-score (98.71%).	2023	EfficientNet-B0 – EfficientNet-B4	98.86%
Padmavathi *et al.,* [14]	A system to classify the types of BT into 4 categories (GT, MT, PT, and no tumor), using EfficientNet architecture. The results indicate the effectiveness of transfer learning when working with limited datasets, achieving an impressive accuracy of 99 percent.	2022	EfficientNet	99%
Du *et al.,* [15]	A system to detect types of BT from an MRI scan. The system is further implemented in a website to increase its accessibility. The system employs transfer learning with EfficientNet to efficiently extract features from brain MRIs, achieving a 98% accuracy in classifying four categories (three tumor types and no tumor)	2021	EfficientNet	98%
Shah *et al.,* [16]	Compared to six deep CNN models and fine-tuned, image enhancement and data augmentation in EfficientNet-B0 achieved the highest accuracy in detecting and classifying BTs using MRI scans. The model attains an impressive 98.87% accuracy for classification and detection, outperforming other models.	2022	EfficientNet-B0	98.87%

Nayak *et al.,* [17]	A dense CNN-based EfficientNet model with min-max normalization is proposed to classify brain MRI images into four categories: GT, MT, PT, and no tumor. This model demonstrates superior accuracy in precise categorization, even with a limited image database, achieving outstanding overall performance. Experimental results validate a testing accuracy of 98.78%.	2022	EfficientNet	98.78%

2. Methodology

This section of the study provides a detailed description of the proposed methodology, the dataset utilized for model training, and the preprocessing steps applied to the dataset. The proposed method contains the following steps: Input, Preprocessing, Training of a model, Tumor detection, and classification as depicted in Figure 2.

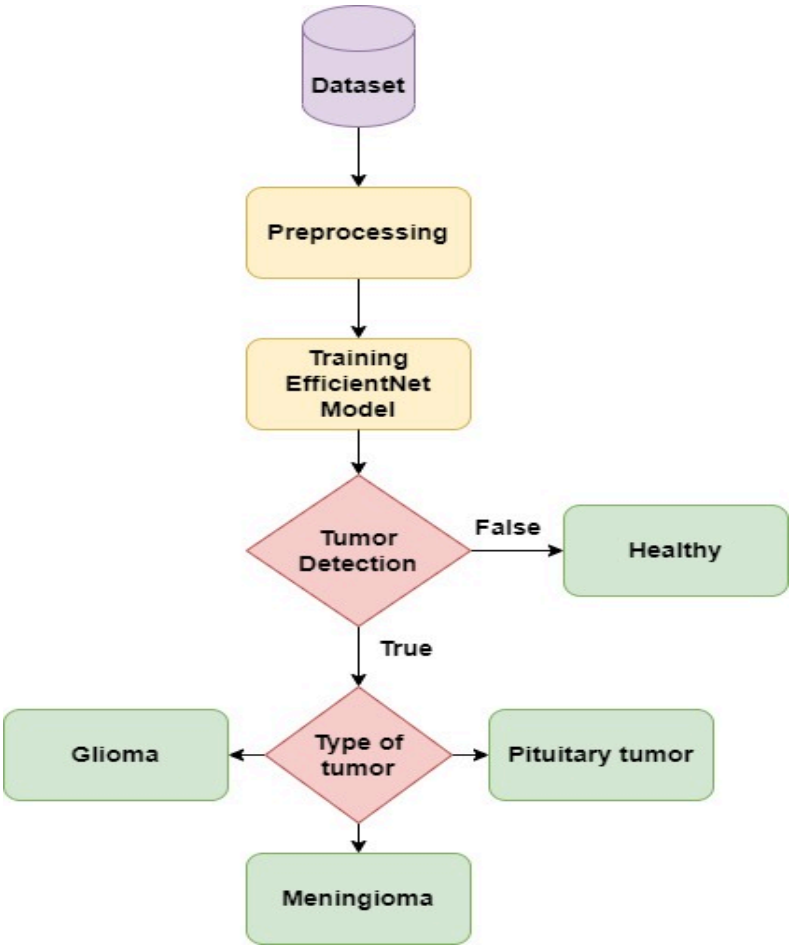

Fig. 2. Proposed model working

2.1 Dataset

The dataset employed for model training comprises around 18,500 MRI scan images, distributed as follows: 6,307 GT, 6,391 MT, and 5,908 PT images (as shown in Figure 3) from the source [18]. This dataset is chosen due to its cleanliness, achieved through a meticulous data-cleaning process. It lacks duplicate images, features proper labelling, and uniform image sizes, reducing the need for extensive preprocessing.

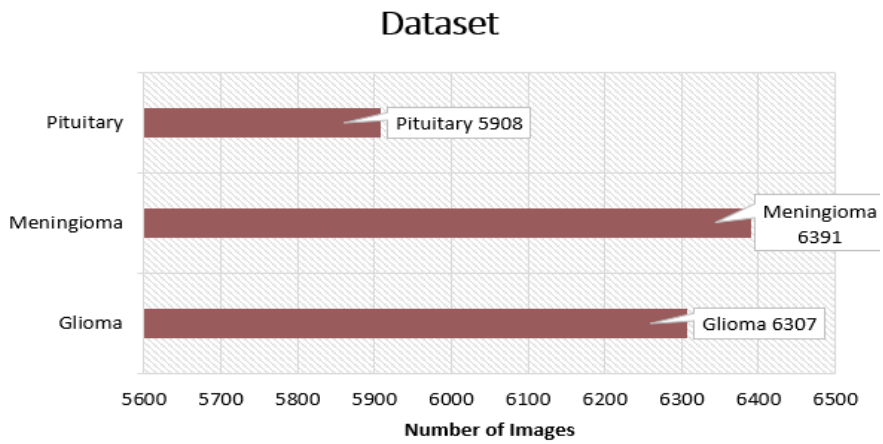

Fig. 3. Data distribution

Furthermore, the dataset has been augmented by the publisher to enhance its robustness and diversity, employing various methods (as shown in Figure 4) such as the conversion of pixels to white or black based on intensity, application of histogram equalization to improve image contrast and detail, rotation of images by predetermined angles (clockwise or anticlockwise), and adjustment of image luminosity by adding or removing intensity values.

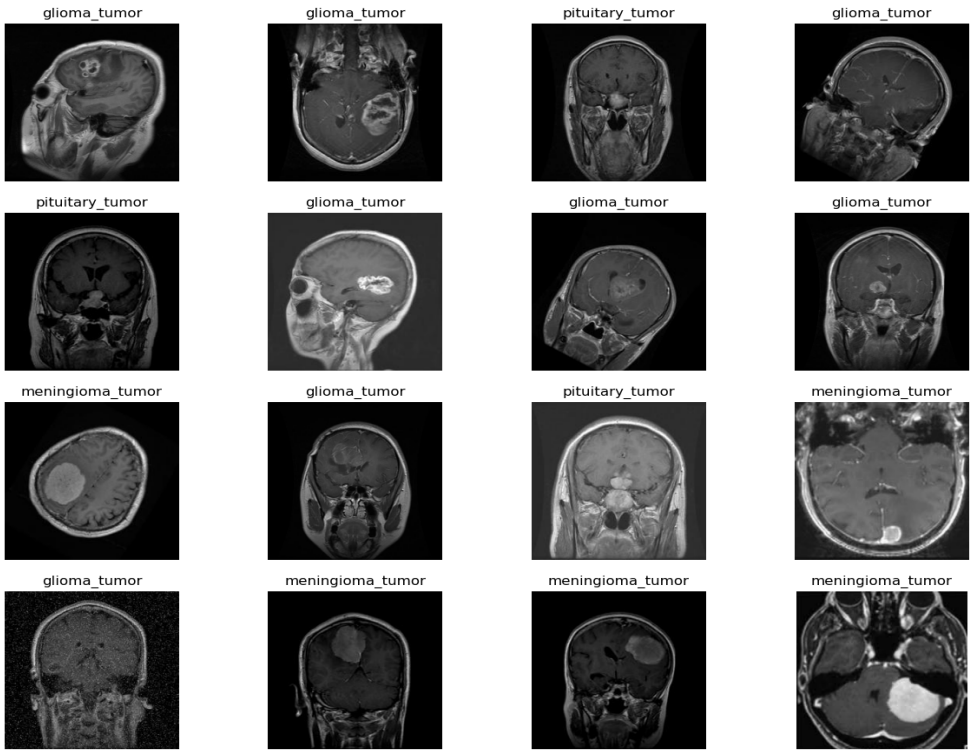

Fig. 4. Some images from the dataset with respective class

2.2 Preprocessing

In the field of image processing, a subset of computer vision, various methods are employed to manipulate and analyze digital images. These techniques involve the application of mathematical or

statistical procedures to alter images and are utilized in various applications, including digital photography, satellite imagery, and medical imaging. Some common image-processing techniques include contrast enhancement, image resizing, noise reduction, segmentation, color correction, and feature extraction [19]. Regarding dataset preprocessing, several steps were undertaken, including feature-wise centering and standard deviation normalization. Horizontal flipping was enabled, and specific values were set: a width shift range, and height shift range of 0.2, and a rotation range of 20 degrees.

Training, validation, and test sets are three separate groups into which the data is divided throughout the dataset preparation step. The test set is used to gauge the efficacy and performance of the trained model, while the training set is used to develop the model and the validation set is used to evaluate and verify the training procedure. Due to this division, the machine learning model may be thoroughly trained, validated, and evaluated. The distribution is shown in Figure 5. The study employs two activation functions: Softmax and ReLU (Rectified Linear Unit).

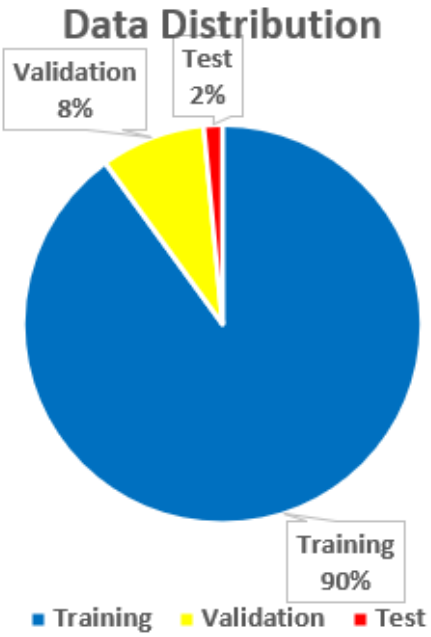

Fig. 5. Train, validate, and test distribution

Softmax: In deep learning, the Softmax activation function is used to transform neural network outputs into probabilities. It's represented by Eq. (1), where SM represents Softmax, ezi represents the exponential of the input vector, and ezj corresponds to the exponential of the output vector.

$$SM = e^{zi} / \sum_{j=1} e^{zj} \tag{1}$$

ReLU (Rectified Linear Unit): ReLU is a popular activation function in neural networks. It produces a non-linear output by replacing all negative inputs with zero. The vanishing gradient issue is alleviated in part by this function. The ReLU function is defined in Eq. (2), where x is the input, and f(x) is the output of the activation function.

$$f(x) = \max(0, x) \tag{2}$$

If the input of the activation function (x) is greater than 0, the output is x. However, if the input is less than 0, the output is set to 0.

ADAM: The optimizer utilized in the model is ADAM (adaptive moment estimation), a well-established algorithm in the realm of deep neural networks known for producing robust results efficiently. Adam is particularly recommended when dealing with large datasets. Calculating the parameters of the Adam optimizer involves determining the mean of gradients and the mean of squared gradients, as depicted in Eq. (3) and Eq. (4).

$$m_t = \beta_1 \times m_{t-1} + g_t \times (1 - \beta_1) \tag{3}$$

$$v_t = \beta_2 \times v_{t-1} + g_t^2 \times (1 - \beta_2) \tag{4}$$

In the given context, mt refers to the first moment estimate at iteration t, vt represents the second moment estimate at iteration t, and gt signifies the gradient at iteration t. Parameters β1 and β2 stand for the exponential decay rates used in the moving average calculations. Once the first and second moments are computed, the bias-corrected first moment estimate and second-moment estimate are calculated, as indicated in Eq. (5) and Eq. (6).

$$\widehat{m_t} = m_t / 1 - \beta_1^t \tag{5}$$

$$\widehat{v_t} = v_t / 1 - \beta_2^t \tag{6}$$

Finally using bias-corrected first and second-moment estimates, parameters are calculated as shown in Eq. (7).

$$x_{t+1} = x_t - \frac{\eta}{\sqrt{\widehat{v_t}} + \epsilon} \times \widehat{m_t} \tag{7}$$

Where xt is the parameter at iteration t, η is the learning rate, and ε is a small constant added to avoid division by 0 [20].

2.3 Model

The implementation incorporates a range of EfficientNet models, including EfficientNet-B0 to EfficientNet-B7. These models are used to explore their performance in various aspects of the research. EfficientNet is a deep neural network architecture introduced by Google in 2019, primarily designed for efficient image classification tasks. It employs a compound scaling technique to simultaneously optimize multiple dimensions, yielding models that are computationally efficient while maintaining high accuracy [21]. The EfficientNet family encompasses models ranging from B0 to B7, which find applications in tasks such as image classification, object detection, segmentation, and various other computer vision challenges. This versatility makes EfficientNet a valuable resource for practitioners in the field of deep learning [22].

The architecture of EfficientNet comprises a baseline network (as shown in Figure 6), known as EfficientNet-B0, and a series of scaled variants, denoted as EfficientNet-B1, B2, B3, and so on, with progressively increasing values of ϕ (depth, width, and resolution combined in a single coefficient). These larger variants typically include more layers, more channels, and higher-resolution input data, allowing them to handle more complex tasks and achieve higher levels of performance [23].

Fig. 6. EfficientNet base architecture

3. Results

This section provides the experimental results obtained by assessing the model's performance under various parameter settings. Additionally, graphical representations are included to visually illustrate and enhance the comprehension of the results.

3.1 EfficientNet-B0

Initially, prior to any tuning, the model underwent training for 2 epochs, thus led to a validation accuracy of 82.08%, indicating that the model correctly classified roughly 82.08% of the validation dataset, with a validation loss of 0.4411, demonstrating how closely the model's predictions aligned with the actual labels. A visual representation of these values per epoch is shown in Figure 7. Following the tuning process, the model was trained for an additional 3 epochs, during which it attained a validation accuracy of 94.94% and a validation loss of 0.1314. The graphical representation of these values for each epoch is shown in Figure 8.

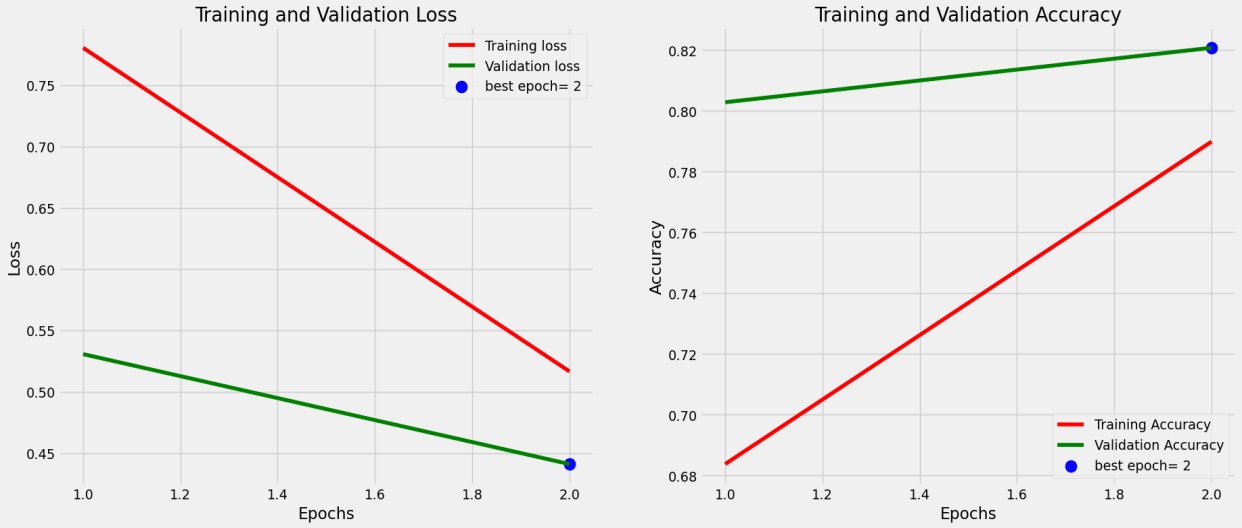

Fig. 7. Graphs displaying the loss and accuracy trends for an EfficientNet-B0 model

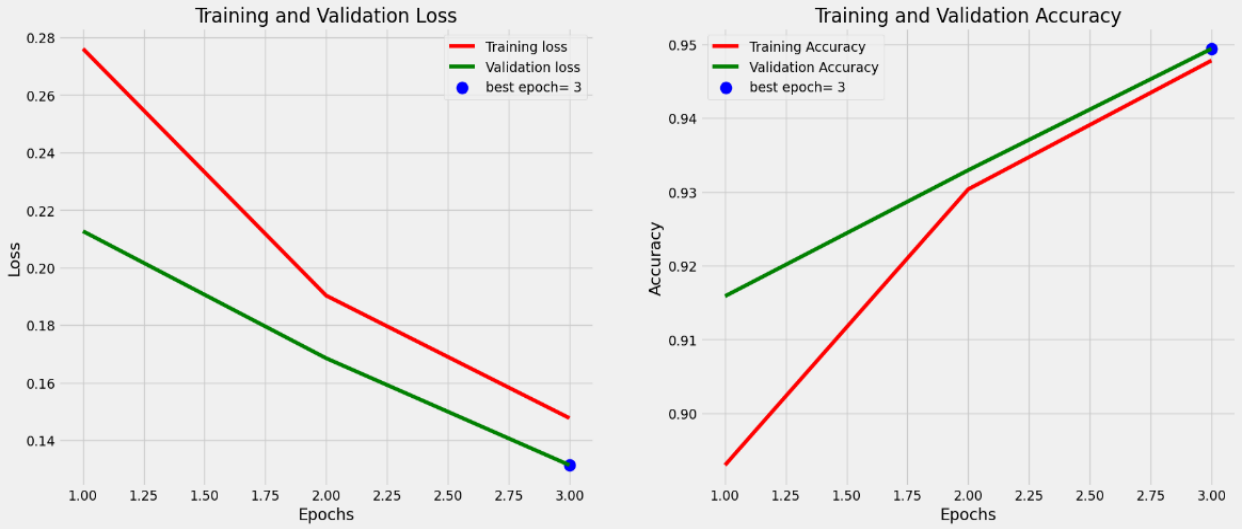

Fig. 8. Graphs depicting the loss and accuracy changes of an optimized EfficientNet-B0 model

3.2 EfficientNet-B1

The model underwent training for 2 epochs initially, thus yielding a validation accuracy of 84.69%, along with a validation loss of 0.4023. The visual representation of these values per epoch is shown in Figure 9. Following the tuning process, the model was trained for an additional 3 epochs, during which it attained a validation accuracy of 96.27% with a validation loss of 0.1219. The graphical representation of these values for each epoch is presented in Figure 10.

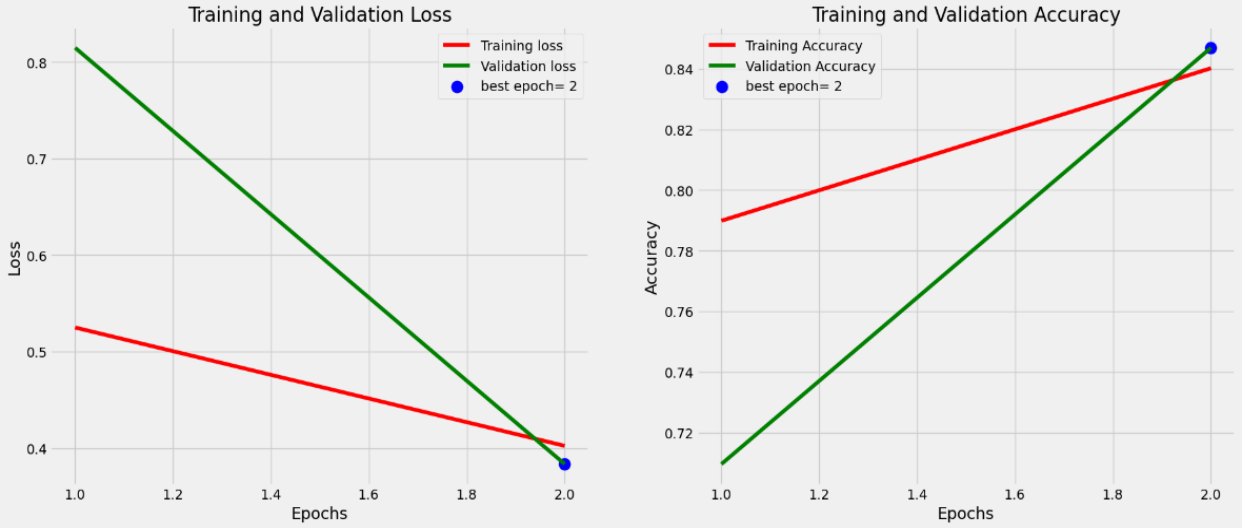

Fig. 9. Graphs displaying the loss and accuracy trends for an EfficientNet-B1 model

Fig. 10. Graphs depicting the loss and accuracy changes of an optimized EfficientNet-B1 model

3.3 EfficientNet-B2

In this, before any tuning, the model underwent training for 2 epochs, thus leading to a validation accuracy of 85.90% and a validation loss of 0.3520. The visual representation of these values per epoch is shown in Figure 11. Following the tuning process, the model was trained for an additional 3 epochs, during which it accomplished a validation accuracy of 96.58% with a validation loss of 0.0988. The graphical representation of these values for each epoch is in TablTaure 12.

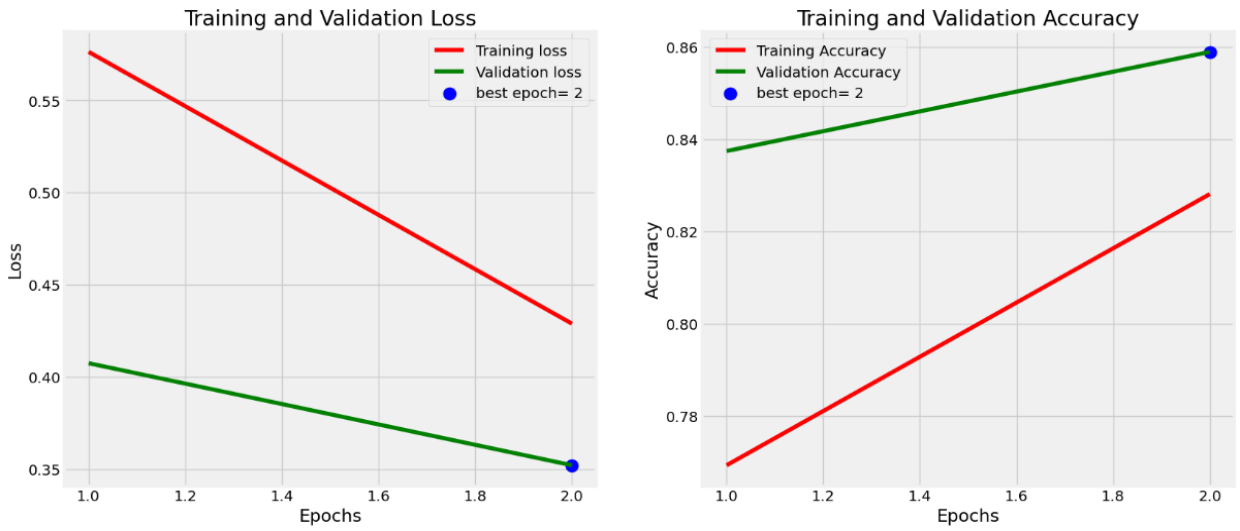

Fig. 11. Graphs displaying the loss and accuracy trends for an EfficientNet-B2 model

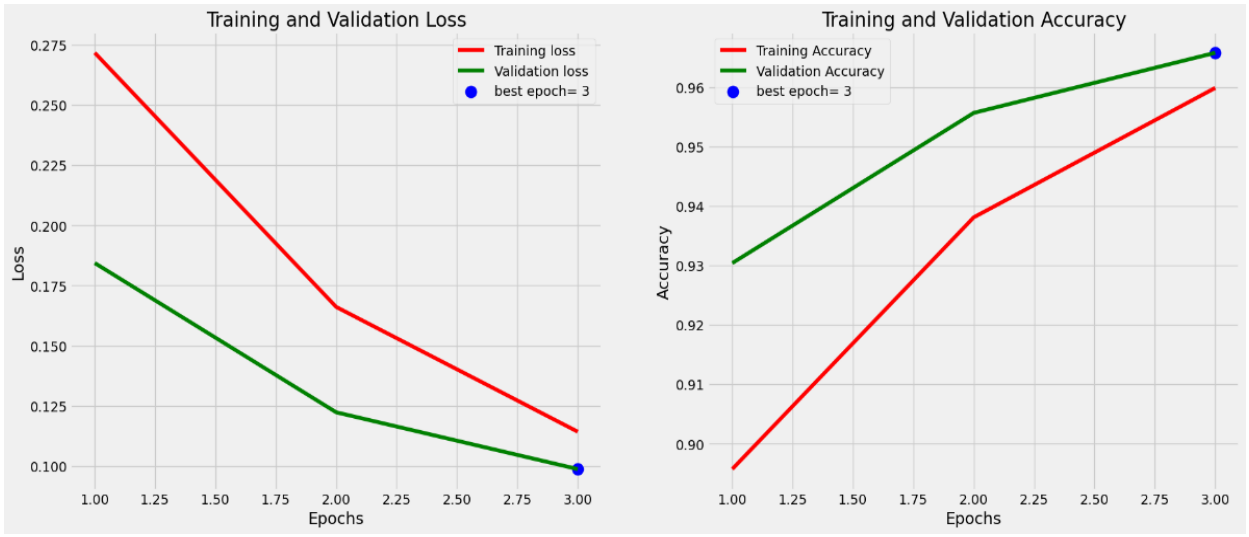

Fig. 12 Graphs depicting the loss and accuracy changes of an optimized EfficientNet-B2 model

3.4 EfficientNet-B3

In this, prior to any tuning, the model underwent training for 3 epochs leading to a validation accuracy of 81.97% and a validation loss of 0.4176. Following the tuning process, the model was trained for an additional 5 epochs, during which it attained a validation accuracy of 97.72% along with a validation loss of 0.0703. The visual representation of these values per epoch and the graphical representation of these values for each epoch are shown in Figure 13 and Figure 14 respectively.

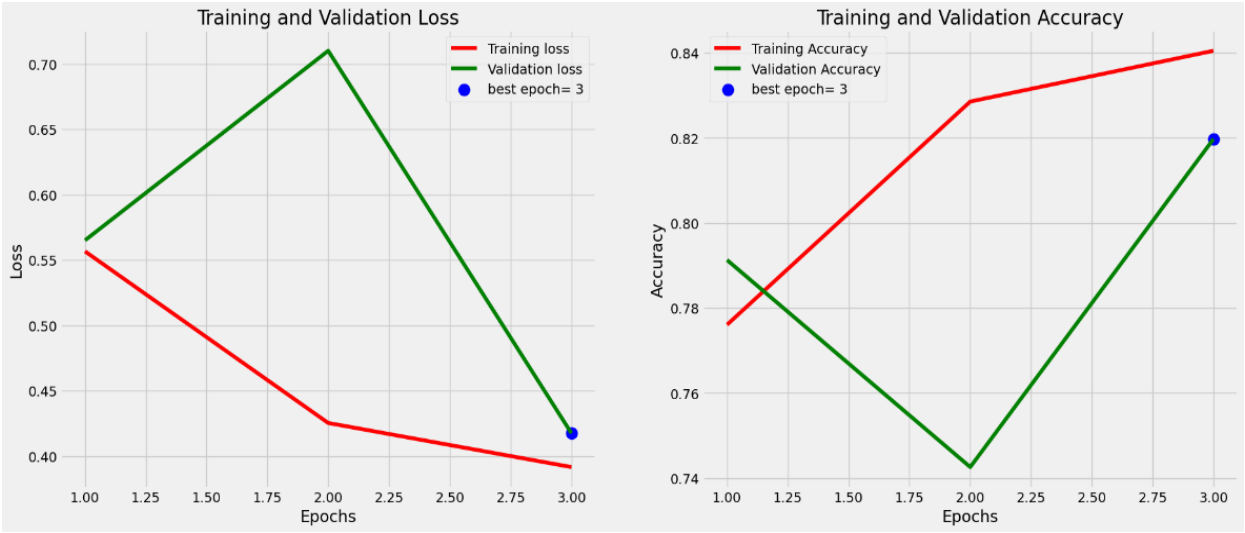

Fig. 13. Graphs displaying the loss and accuracy trends for an EfficientNet-B3 model

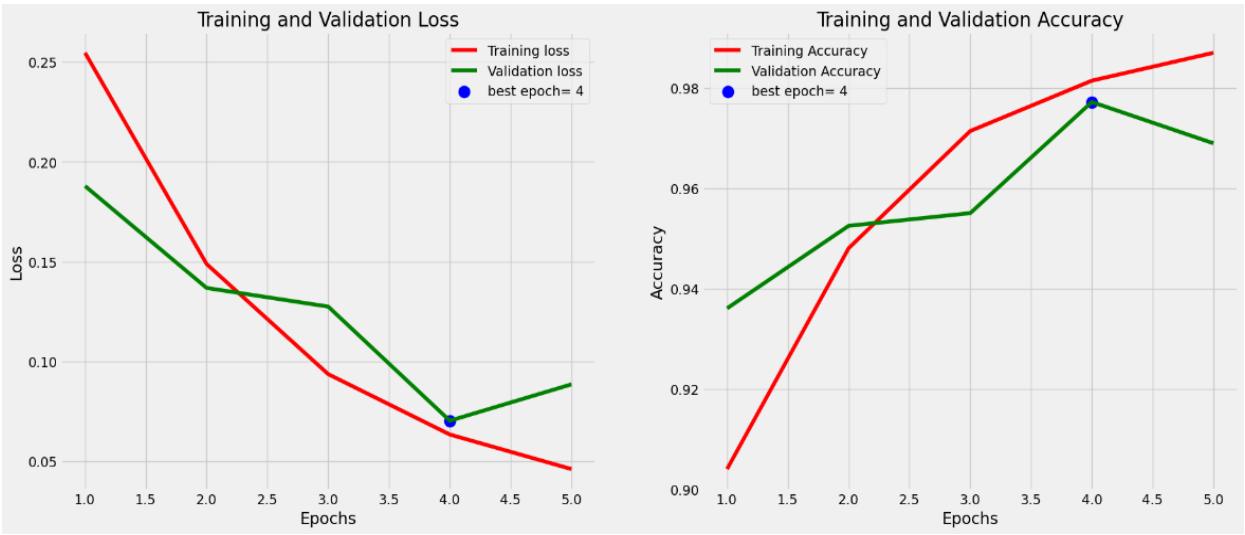

Fig. 14. Graphs depicting the loss and accuracy changes of an optimized EfficientNet-B3 model

3.5 EfficientNet-B4

The model underwent training for 3 epochs, leading to a validation accuracy of 85.07% and a validation loss of 0.3899. After the tuning process, the model was trained for an additional 5 epochs, during which it accomplished a validation accuracy of 98.88% with a validation loss of 0.0433. The visual representation of these values per epoch and the graphical representation of these values for each epoch are shown in Figure 15 and Figure 16 respectively.

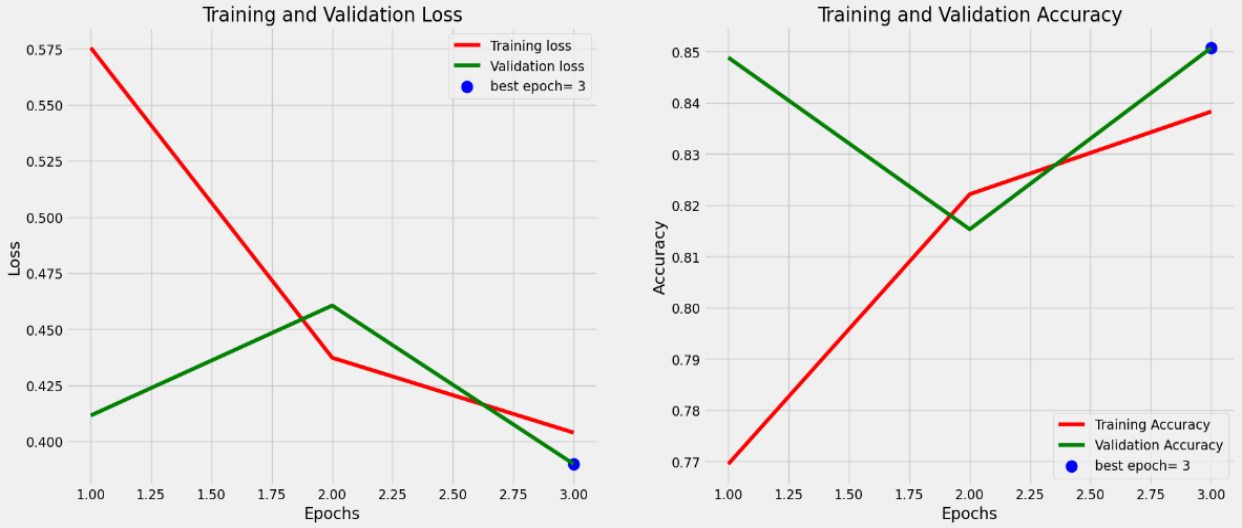

Fig. 15. Graphs displaying the loss and accuracy trends for an EfficientNet-B4 model

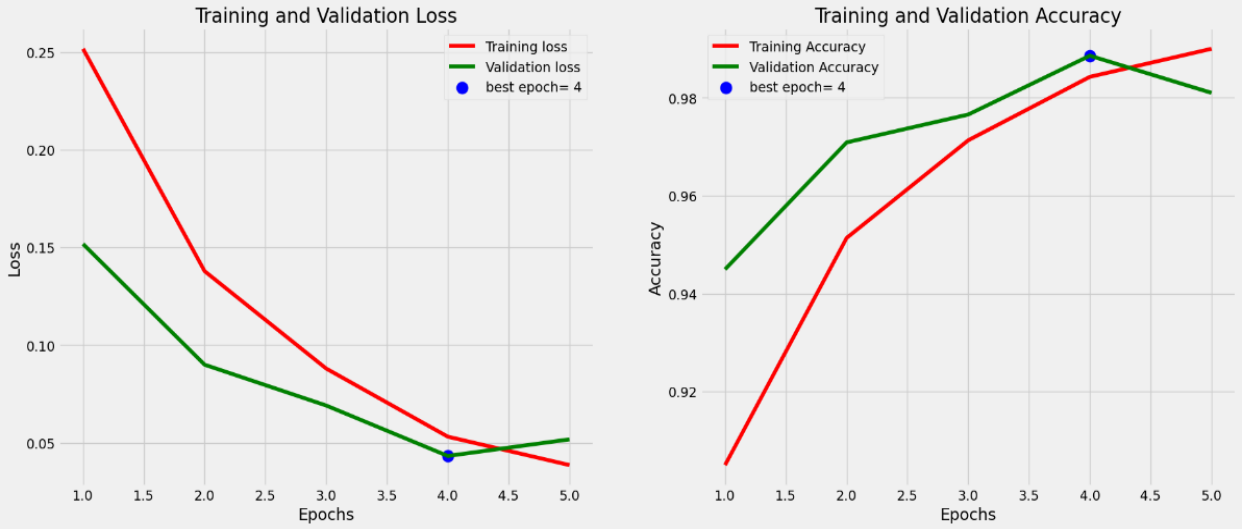

Fig. 16. Graphs depicting the loss and accuracy changes of an optimized EfficientNet-B4 model

3.6 EfficientNet-B5

In this, the model underwent training for 3 epochs, this led to a validation accuracy of 86.46% and a validation loss of 0.4150. The visual representation of these values per epoch is shown in Figure 17. Following the tuning process, the model was trained for an additional 5 epochs, during which it attained a validation accuracy of 98.92% with a validation loss of 0.0358. The graphical representation of these values for each epoch is presented in Figure 18.

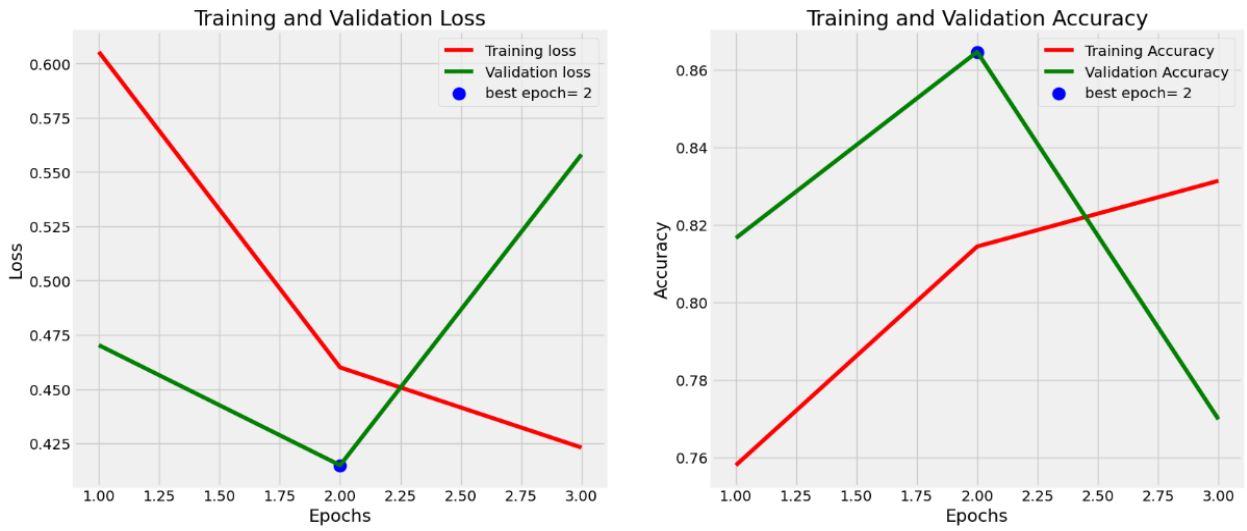

Fig. 17. Graphs displaying the loss and accuracy trends for an EfficientNet-B5 model

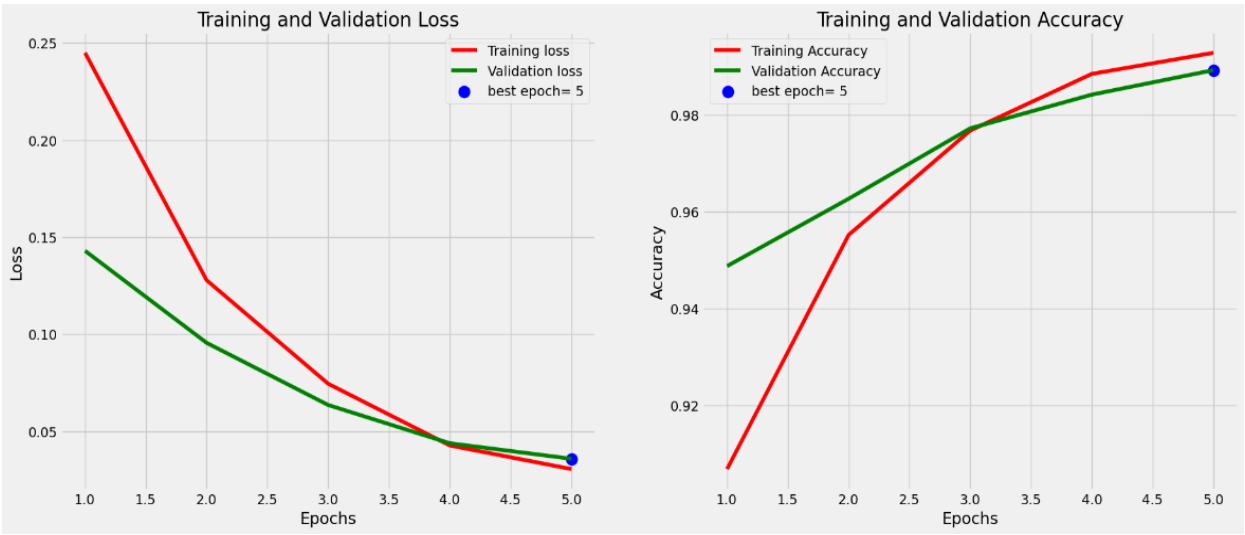

Fig. 18. Graphs depicting the loss and accuracy changes of an optimized EfficientNet-B5 model

3.7 EfficientNet-B6

Initially, prior to any tuning, the model underwent training for 3 epochs, thus resulting in a validation accuracy of 85.26% and a validation loss of 0.3794. Following the tuning process, the model was trained for an additional 5 epochs, during which it accomplished a validation accuracy of 99.05% with a validation loss of 0.0354. The visual representation of these values per epoch and the graphical representation of these values for each epoch are shown in Figure 19 and Figure 20 respectively.

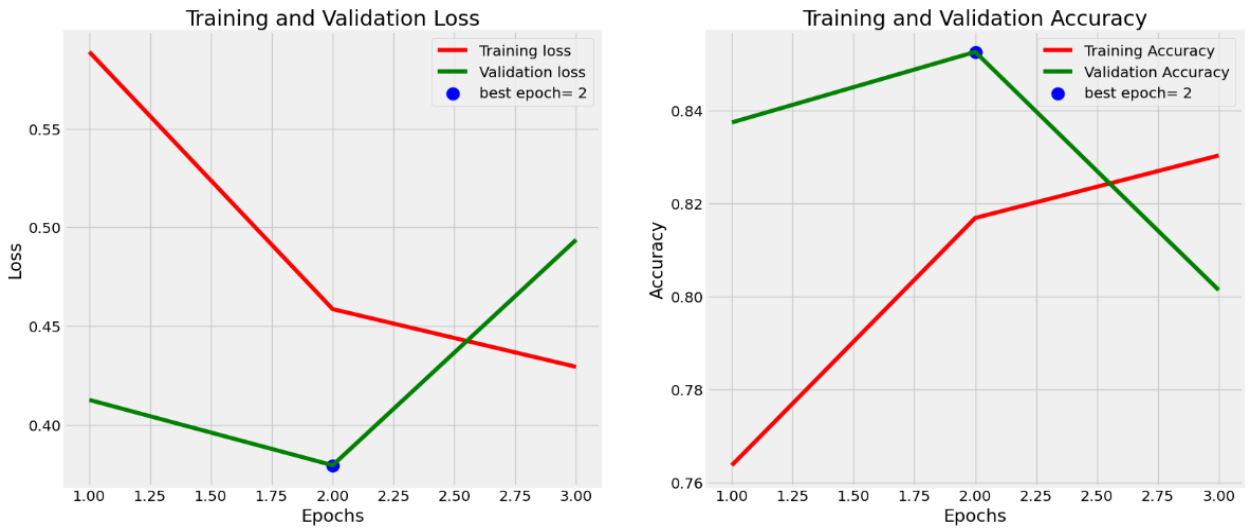

Fig. 19. Graphs displaying the loss and accuracy trends for an EfficientNet-B6 model.

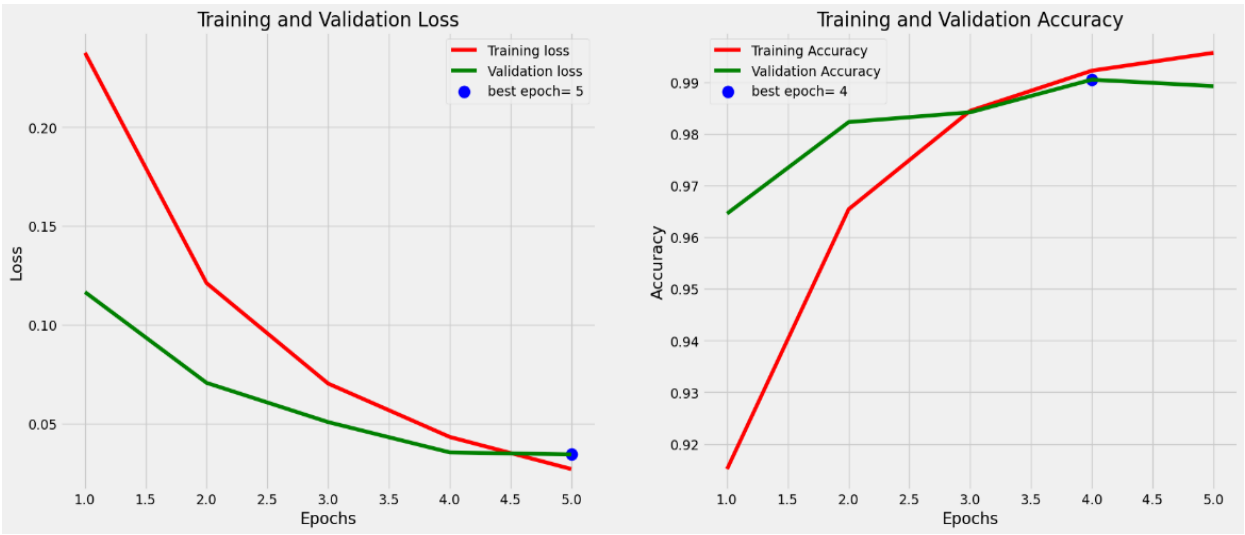

Fig. 20. Graphs depicting the loss and accuracy changes of an optimized EfficientNet-B6 model.

3.8 EfficientNet-B7

The model underwent training for 3 epochs prior to any tuning, this led to a validation accuracy of 85.62% and a validation loss of 0.3780. The visual representation of these values per epoch is shown in Figure 21. Following the tuning process, the model was trained for an additional 5 epochs, during which it attained a validation accuracy of 98.99% with a validation loss of 0.0274. The graphical representation of these values for each epoch is presented in Figure 22. Table 2 presents a comparison of all model results.

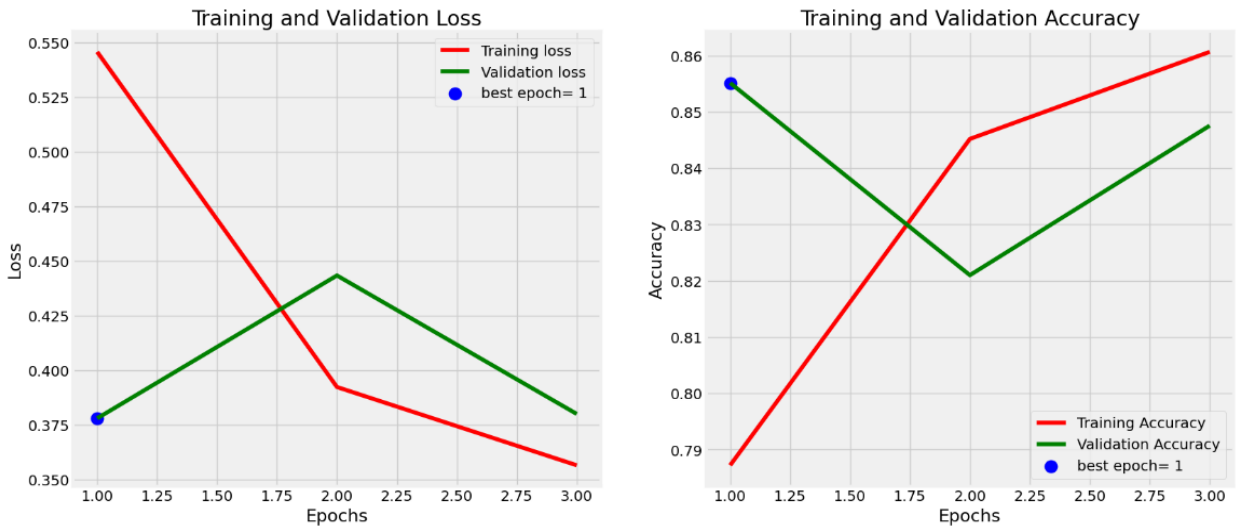

Fig. 21. Graphs displaying the loss and accuracy trends for an EfficientNet-B7 model.

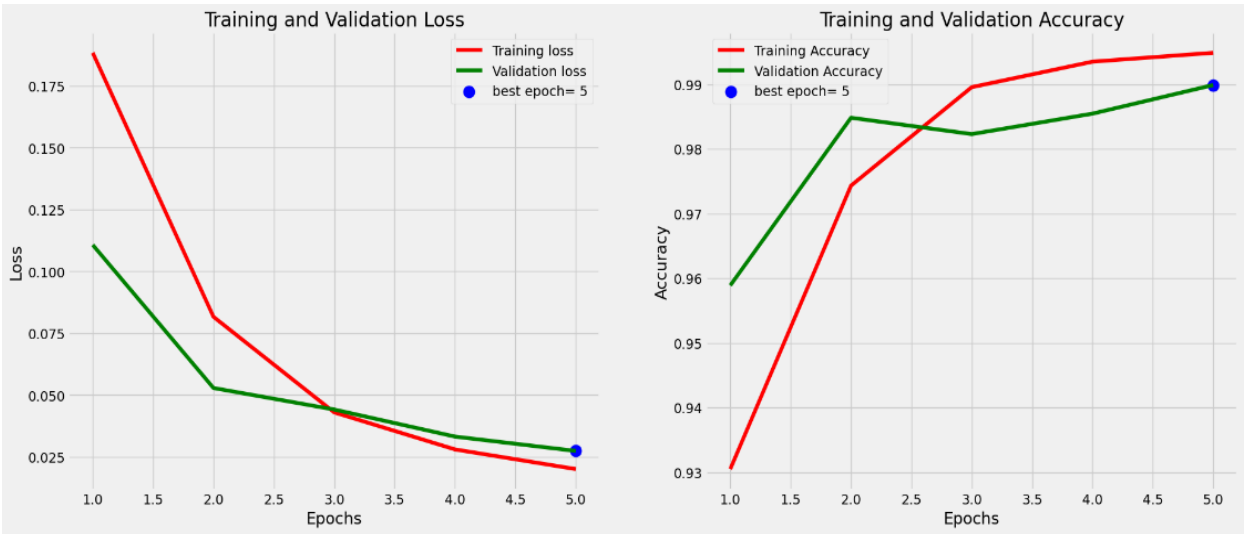

Fig. 22. Graphs depicting the loss and accuracy changes of an optimized EfficientNet-B7 model.

Table 2
Evaluation Results of models used in the study

Model	Tuning	Number of epochs	Training Loss	Training Accuracy	Validation Loss	Validation Accuracy
EfficientNet-B0	Before	1	0.5450	78.02%	0.5267	78.81%
		2	0.4036	83.77%	0.6245	72.74%
	After	1	0.2760	89.30%	0.2127	91.59%
		2	0.1903	93.04%	0.1695	93.30%
		3	0.1477	94.78%	0.1314	94.94%
EfficientNet-B1	Before	1	0.5250	78.99%	0.8149	70.97%
		2	0.4023	84.02%	0.3834	84.69%
	After	1	0.2715	89.54%	0.2384	90.07%
		2	0.1677	93.92%	0.1305	95.19%
		3	0.1219	95.88%	0.1005	96.27%
EfficientNet-B2	Before	1	0.5763	76.93%	0.4074	83.74%
		2	0.4288	82.81%	0.3520	85.90%

	After	1	0.2716	89.57%	0.1844	93.04%
		2	0.1661	93.81%	0.1224	95.57%
		3	0.1144	95.99%	0.0988	96.58%
EfficientNet-B3	Before	1	0.5567	77.61%	0.5651	79.13%
		2	0.4254	82.85%	0.7101	74.26%
		3	0.3916	84.05%	0.4176	81.97%
	After	1	0.2546	90.41%	0.1879	93.61%
		2	0.1488	94.81%	0.1368	95.26%
		3	0.0936	97.15%	0.1274	95.51%
		4	0.0633	98.15%	0.0703	97.72%
		5	0.0460	98.70%	0.0885	96.90%
EfficientNet-B4	Before	1	0.5755	76.95%	0.4115	84.88%
		2	0.4373	82.22%	0.4606	81.53%
		3	0.4049	83.83%	0.3899	85.07%
	After	1	0.2517	90.50%	0.1518	94.50%
		2	0.1379	95.14%	0.0900	97.09%
		3	0.0880	97.13%	0.0691	97.66%
		4	0.0531	98.43%	0.0433	98.88%
		5	0.0386	99.00%	0.0518	98.10%
EfficientNet-B5	Before	1	0.6053	75.79%	0.4703	81.66%
		2	0.4600	81.44%	0.4150	86.46%
		3	0.4231	83.14%	0.5581	76.98%
	After	1	0.2450	90.68%	0.1430	94.88%
		2	0.1278	95.52%	0.0955	96.27%
		3	0.0744	97.68%	0.0635	97.72%
		4	0.0427	98.85%	0.0438	98.42%
		5	0.0305	99.28%	0.0358	98.92%
EfficientNet-B6	Before	1	0.5889	76.37%	0.4125	83.74%
		2	0.4585	81.69%	0.3794	85.26%
		3	0.4293	83.03%	0.4937	80.14%
	After	1	0.2377	91.51%	0.1165	96.46%
		2	0.1211	96.54%	0.0706	98.23%
		3	0.0702	98.45%	0.0507	98.42%
		4	0.0432	99.22%	0.0354	99.05%
		5	0.0269	99.57%	0.0344	98.92%
EfficientNet-B7	Before	1	0.5458	78.72%	0.3780	85.62%
		2	0.3923	84.52%	0.4434	82.10%
		3	0.3565	86.07%	0.3800	84.76%
	After	1	0.1884	93.0%	0.1107	95.89%
		2	0.0816	97.43%	0.0528	98.48%
		3	0.0430	98.95%	0.0441	98.23%
		4	0.0280	99.35%	0.0332	98.55%
		5	0.0201	99.49%	0.0274	98.99%

The model's efficiency is evaluated in terms of accuracy using Eq. (8), where the abbreviations correspond to the following: FP (False Positive), TN (True Negative), TP (True Positive), and FN (False Negative).

$$Accuracy = TP + TN/FN + FP + TN + TP \quad (8)$$

Following the training and validation phases, the model is subjected to testing using the test class of the dataset, consisting of 280 images. During the testing process, the model predicts the outputs, generates a Confusion Matrix (CM), and calculates the f-score and precision table. A CM serves as a valuable instrument for evaluating the effectiveness of a classification algorithm or model. It provides

a structured summary in table format that showcases the model's predictions and their outcomes, showing how many instances of each class were correctly classified and how many were incorrectly classified. This matrix aids in understanding the model's accuracy, precision, recall, and other important metrics, enabling a thorough evaluation of its performance [24]. The figures of the confusion matrices for EfficientNet-B0 to EfficientNet-B3 are displayed in Figure 23, with each subfigure labelled from (a) to (d) and from EfficientNet-B4 to EfficientNet-B7 are in Figure 24(a-d) accordingly. These matrices provide insights into the model's performance in terms of classification accuracy and errors.

Figure 23(a-d) illustrates the performance of the EfficientNet-B0 to EfficientNet-B3 models in predicting BT images respectively. Out of 280 images, the model correctly predicted 269 images for EfficientNet-B0, out of 280 images, the model correctly predicted 274 images for EfficientNet-B1, out of 280 images, the model correctly predicted 275 images for EfficientNet-B2, and out of 280 images, the model correctly predicted 274 images for EfficientNet-B3, which are represented in the TP and TN parts of the CM. However, there were 11 images that the model did not predict correctly in EfficientNet-B0, 6 images predicted incorrectly in EfficientNet-B1, 5 images predicted incorrectly in EfficientNet-B2, and 6 images predicted incorrectly in EfficientNet-B3 indicated in the FP and FN parts of the CM.

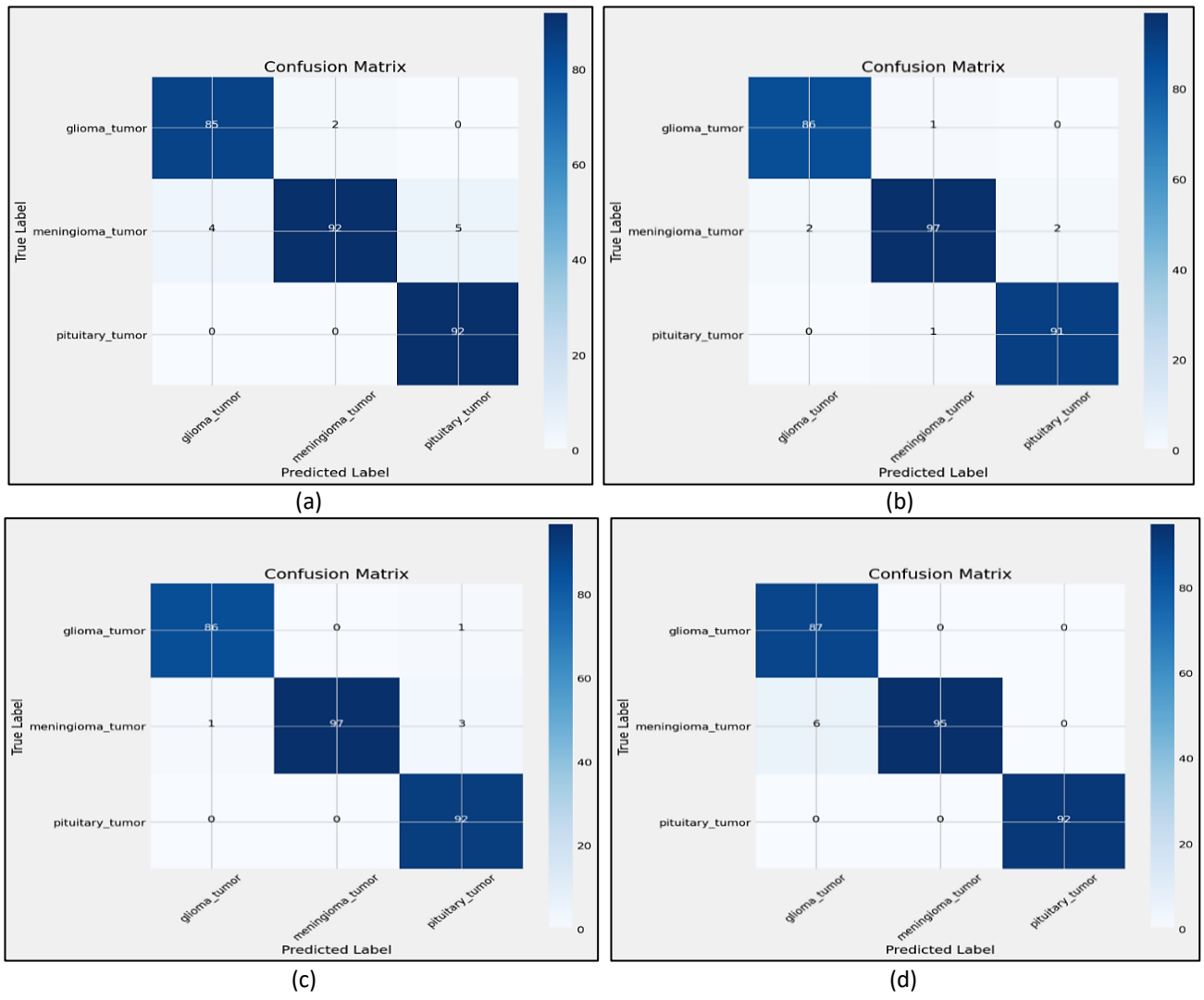

Fig. 23. (a) CM of EfficientNet-B0 (b) CM of EfficientNet-B1 (c) CM of EfficientNet-B2 (d) CM of EfficientNet-B3

Specifically, among these in Figure 23 misclassified images are

I. In EfficientNet-B0, 2 GT images were incorrectly predicted as MT, 4 MT images were mistakenly classified as GT, and 5 MT images were inaccurately classified as PTs.
II. In EfficientNet-B1, 2 GT images were incorrectly predicted as MT, 2 MT images were mistakenly classified as GT, 2 MT images were inaccurately classified as PTs, and 1 PT image was mistakenly classified as MT.
III. In EfficientNet-B2, 1 GT image was incorrectly predicted as PT, 1 MT image was mistakenly classified as GT, and 3 MT images were inaccurately classified as PTs.
IV. In EfficientNet-B3, 6 MT images were mistakenly classified as GT.

Figure 24(a-d) illustrates the performance of the EfficientNet-B4 to EfficientNet-B7 models in predicting BT images respectively. Out of 280 images, the model correctly predicted 277 images in EfficientNet-B4, out of 280 images, the model correctly predicted 279 images in EfficientNet-B5, out of 280 images, the model correctly predicted 276 images in EfficientNet-B6, and out of 280 images, the model correctly predicted 279 images in EfficientNet-B7 which are represented in the TP and TN part of the CM. However, there were 3 images that the model did not predict correctly in EfficientNet-B4, 1 image was predicted incorrectly in EfficientNet-B5, 4 images were predicted incorrectly in EfficientNet-B6, and 1 image was predicted incorrectly in EfficientNet-B7, indicated in the FP and FN part of the CM.

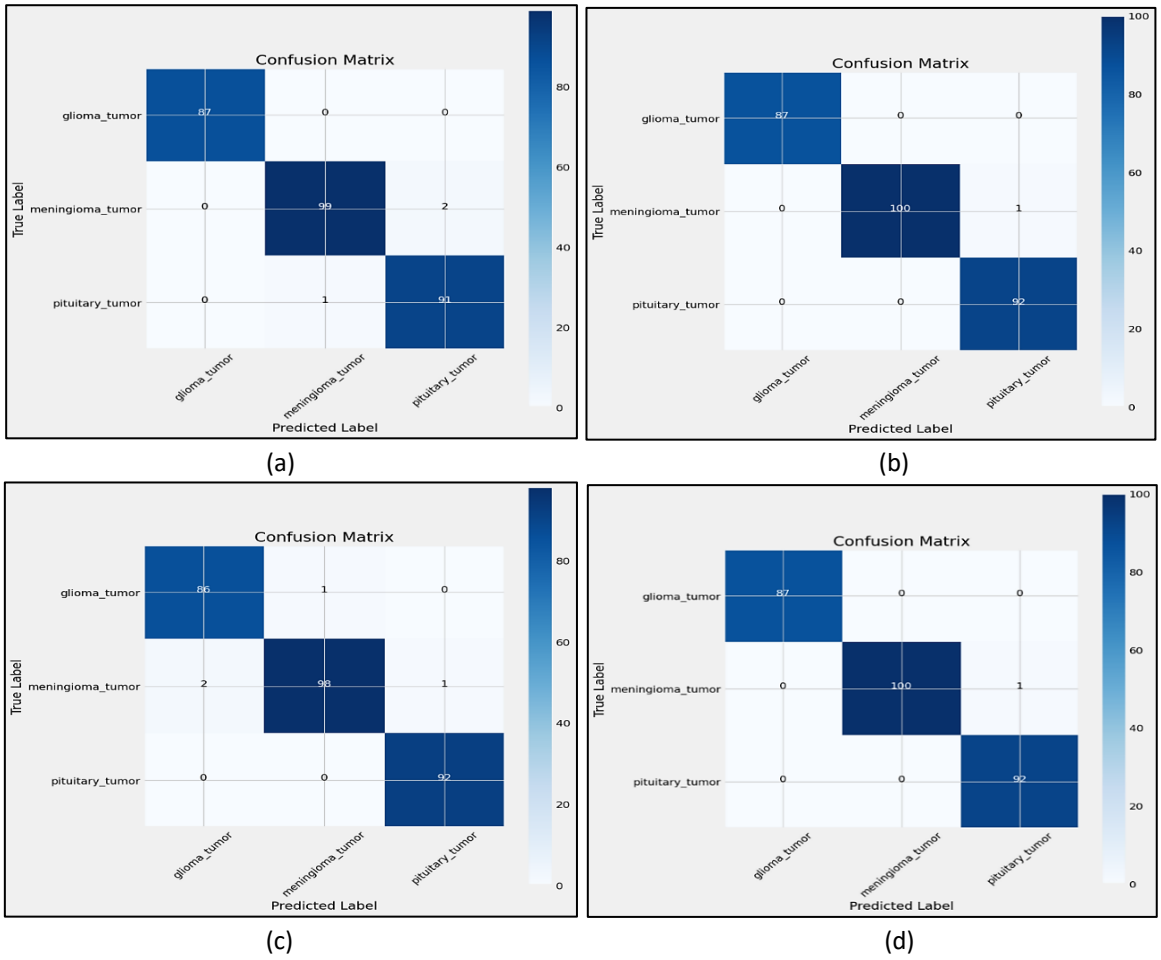

Fig. 24. (a) CM of EfficientNet-B4 (b) CM of EfficientNet-B5 (c) CM of EfficientNet-B6 (d) CM of EfficientNet-B7

Specifically, among these CMs in Figure 24, the misclassified images are

i. In EfficientNet-B4, 2 MT images were inaccurately classified as PTs, 1 PT image was mistakenly classified as MT.
ii. In EfficientNet-B5, 1 MT image was inaccurately classified as PTs.
iii. In EfficientNet-B6, 1 GT image was incorrectly predicted as MT, 2 MT images were mistakenly classified as GT, 1 MT image was inaccurately classified as PTs.
iv. In EfficientNet-B7, 1 MT image was inaccurately classified as PTs.

The summary of the prediction results for all the models can be found in Table 3, which provides a comprehensive overview of the assessment of each model's effectiveness based on accuracy, precision, recall, and F1-score. This table allows for a quick comparison of how well each model performed in classifying BT images.

Table 3
Prediction table of all the models

Model	Classes	Precision	Recall	F1 Score
EfficientNet-B0	GT	0.96	0.98	0.97
	MT	0.98	0.91	0.94
	PT	0.95	1.00	0.97
EfficientNet-B1	GT	0.98	0.99	0.98
	MT	0.98	0.96	0.97
	PT	0.98	0.99	0.98
EfficientNet-B2	GT	0.99	0.99	0.99
	MT	1.00	0.96	0.98
	PT	0.96	1.00	0.98
EfficientNet-B3	GT	0.94	1.00	0.97
	MT	1.00	0.94	0.97
	PT	1.00	1.00	1.00
EfficientNet-B4	GT	1.00	1.00	1.00
	MT	0.99	0.98	0.99
	PT	0.98	0.99	0.98
EfficientNet-B5	GT	1.00	1.00	1.00
	MT	1.00	0.99	1.00
	PT	0.99	1.00	0.99
EfficientNet-B6	GT	0.98	0.99	0.98
	MT	0.99	0.97	0.98
	PT	0.99	1.00	0.99
EfficientNet-B7	GT	1.00	1.00	1.00
	MT	1.00	0.99	1.00
	PT	0.99	1.00	0.99

The formulas to calculate common metrics from a CM include, precision, recall, specificity, and F1 score are shown in Eq. (9), Eq. (10), Eq. (11), and Eq. (12) respectively.

$$Precision = {TP}/{TP + FP} \tag{9}$$

$$Recall = {TP}/{TP + FN} \tag{10}$$

$$Specificity = {TN}/{TN + FP} \tag{11}$$

$$F1 - Score = 2X(Precision\ X\ Recall)/(Precision + Recall) \tag{12}$$

After completing all the necessary steps, including training, validation, and testing, the test accuracy of each model is calculated. These test accuracies for all the models are typically presented in Table 4. This table provides a clear comparison of how well each model performed when tested on a separate dataset, allowing researchers and practitioners to assess their effectiveness in classifying BT images.

Table 4
Test accuracy of all the models

Model	Test Loss	Test Accuracy	F1 Score
EfficientNet-B0	0.12305	96.07%	0.9610
EfficientNet-B1	0.07715	97.86%	0.9788
EfficientNet-B2	0.07316	98.21%	0.9823
EfficientNet-B3	0.08936	97.86%	0.9786
EfficientNet-B4	0.03768	98.93%	0.9896
EfficientNet-B5	0.02848	99.64%	0.9965
EfficientNet-B6	0.03794	98.57%	0.9858
EfficientNet-B7	0.01540	99.64%	0.9965

4. Conclusions

A robust BT detection system leveraging the EfficientNet model is presented using SoftMax, ReLu activation function, and ADAM optimizer. The investigation entailed a thorough assessment of the performance of eight distinct variants of the EfficientNet model, spanning from B0 to B7. The outcomes of the study underscored the exceptional potential of the EfficientNet architecture in the precise differentiation and classification of BT types. The study has produced remarkable results, highlighting the superior performance of EfficientNet-B5 and EfficientNet-B7 as the top-performing models. These two models displayed an exceptional accuracy rate of 99.64%, marking a significant milestone in BT detection. This achievement underscores the substantial progress made in the domain of medical image analysis and reaffirms the effectiveness of deep learning models, particularly the EfficientNet architecture, in addressing critical healthcare challenges. In summary, the study emphasizes the transformative potential of advanced deep learning models like EfficientNet in reshaping healthcare practices, particularly in the crucial task of early and precise detection of life-threatening conditions like BTs. The exceptional accuracy rates attained by these models have the capacity to bring about substantial improvements in patient care, ultimately leading to better outcomes and enhanced quality of life for individuals grappling with BTs. This research lays the foundation for continued exploration and seamless integration of cutting-edge technology into clinical environments, driving forward the boundaries of medical science and patient-centered care.

Future applications of deep learning technology and models like EfficientNet for brain tumor identification are both exciting and diverse. The following are some crucial areas where more improvements and developments might be anticipated

i. Enhanced accuracy: Further study will probably result in even greater rates of brain tumor detection efficiency. Performance will be enhanced by optimizing hyperparameters, fine-tuning models, and increasing datasets [25].
ii. Early detection: Focused efforts shall be made to identify brain tumors at even earlier stages, allowing for more efficient therapies and maybe improved outcomes for patients [26].
iii. Multi-class classification: In the future, technologies could be able to divide brain tumors into more precise subgroups, giving doctors in-depth knowledge for individualized treatment regimens [27].

iv. Real-time detection: The creation of real-time brain tumor detection devices may fundamentally alter surgical procedures by enabling surgeons to make well-informed judgments [28].
v. Radiologists and other medical professionals may benefit from immediate analysis and interpretation of data if MRI and other imaging technologies were integrated seamlessly.
vi. Quantitative evaluation: As systems develop, they may eventually provide numerical information on tumor size, pace of development, and response to therapy, assisting in the monitoring of the latter [29].
vii. Genetic analysis: Integrating genetic data might help us understand the hereditary elements that are connected to brain tumors better and, perhaps, develop more precise treatments [30,33].
viii. AI-driven drug discovery: By examining enormous molecular and clinical data sets, AI models may help in the identification of new medications and treatments for the treatment of brain tumors [31,34].
ix. Ethical Considerations: As these systems proliferate, continual attention will be needed to address ethical issues relating to patient data protection, bias reduction, and AI transparency [32,35].

The future of BT detection systems is poised to significantly enhance patient care, elevate medical decision-making, and deepen our comprehension of BTs. Ongoing research and innovative endeavours will propel these advancements, delivering advantages to both patients and the medical field.

Acknowledgement

The authors acknowledge Organizations for the support provided for carrying out the research work in the stipulated time.

References

[1] NIH. "Brain basics: Know your brain." *National Institute of Neurological Disorders and Stroke* (2023).
[2] AANS. "Neurosurgical Conditions and Treatments." *American Association of Neurological Surgeons*.
[3] Binello, Emanuela, and Isabelle M. Germano. "Targeting glioma stem cells: a novel framework for brain tumours." *Cancer science* 102, no. 11 (2011): 1958-1966. https://doi.org/10.1111/j.1349-7006.2011.02064.x
[4] Cancer.Net. "Brain Tumor: Statisctics." *ASCO Knowledge Conquers Cancer* (2023).
[5] Netmeds. "World Brain Tumour Day 2022: Learn about the significance theme and facts."
[6] GLOBUS, JOSEPH H. "Meningiomas: origin, divergence in structure and relationship to contiguous tissues in light of phylogenesis and ontogenesis of the meninges, with suggestion of a simplified classification of meningeal neoplasms." *Archives of Neurology & Psychiatry* 38, no. 4 (1937): 667-712. https://doi.org/10.1001/archneurpsyc.1937.02260220011001
[7] Arafah, B. M., and M. P. Nasrallah. "Pituitary tumors: pathophysiology, clinical manifestations and management." *Endocrine-related cancer* 8, no. 4 (2001): 287-305. https://doi.org/10.1677/erc.0.0080287
[8] Mishra, Shailendra Kumar, Dheeraj Kumar, Gaurav Kumar, and Sujeet Kumar. "Multi-classification of brain MRI using EfficientNet." In *2022 International Conference for Advancement in Technology (ICONAT)*, pp. 1-6. IEEE, 2022.
[9] Mahesh, Abishek, Deeptimaan Banerjee, Ahona Saha, Manas Ranjan Prusty, and A. Balasundaram. "CE-EEN-B0: Contour Extraction Based Extended EfficientNet-B0 for Brain Tumor Classification Using MRI Images." *Computers, Materials & Continua* 74, no. 3 (2023). https://doi.org/10.32604/cmc.2023.033920
[10] Isunuri, B. Venkateswarlu, and Jagadeesh Kakarla. "EfficientNet and multi-path convolution with multi-head attention network for brain tumor grade classification." *Computers and Electrical Engineering* 108 (2023): 108700. https://doi.org/10.1016/j.compeleceng.2023.108700
[11] Goutham, Veeranki, Abdul Sameerunnisa, Sallagundla Babu, and Tugu Bhanu Prakash. "Brain tumor classification using Efficientnet-B0 model." In *2022 2nd International Conference on Advance Computing and Innovative Technologies in Engineering (ICACITE)*, pp. 2503-2509. IEEE, 2022. https://doi.org/10.1109/ICACITE53722.2022.9823526

[12] Mantha, Tejakrishna, and B. Eswara Reddy. "A transfer learning method for brain tumor classification using efficientnet-b3 model." In *2021 IEEE International Conference on Computation System and Information Technology for Sustainable Solutions (CSITSS)*, pp. 1-6. IEEE, 2021. https://doi.org/10.1109/CSITSS54238.2021.9683036
[13] Zulfiqar, Fatima, Usama Ijaz Bajwa, and Yasar Mehmood. "Multi-class classification of brain tumor types from MR images using EfficientNets." *Biomedical Signal Processing and Control* 84 (2023): 104777. https://doi.org/10.1016/j.bspc.2023.104777
[14] Padmavathi, K., Om Sri Rohith Raj Yadav Thalla, Sithagari Sujeeth Reddy, Priyanka Yadlapalli, Thakur Roshan, and Thodupunoori Charan. "Transfer learning using efficientnet for brain tumor classification from mri images." In *2022 International Conference on Computer Communication and Informatics (ICCCI)*, pp. 1-4. IEEE, 2022. https://doi.org/10.1109/ICCCI54379.2022.9740923
[15] Du, Wuhao, Yujie He, Yancheng Li, and Ziqi Wu. "Brain tumor diagnosis using EfficientNet." In *Second IYSF Academic Symposium on Artificial Intelligence and Computer Engineering*, vol. 12079, pp. 18-25. SPIE, 2021. https://doi.org/10.1117/12.2623082
[16] Shah, Hasnain Ali, Faisal Saeed, Sangseok Yun, Jun-Hyun Park, Anand Paul, and Jae-Mo Kang. "A robust approach for brain tumor detection in magnetic resonance images using finetuned efficientnet." *Ieee Access* 10 (2022): 65426-65438. https://doi.org/10.1109/ACCESS.2022.3184113
[17] Nayak, Dillip Ranjan, Neelamadhab Padhy, Pradeep Kumar Mallick, Mikhail Zymbler, and Sachin Kumar. "Brain tumor classification using dense efficient-net." *Axioms* 11, no. 1 (2022): 34. https://doi.org/10.3390/axioms11010034
[18] Hashemi, M. Hossein. "Crystal clean: Brain tumors MRI dataset." (2023).
[19] Bhutanadhu, Hari. "Getting Started with Cloud Security and Its Applications." *Analytics Vidhya* (2023).
[20] Marques, Gonçalo, Deevyankar Agarwal, and Isabel De la Torre Díez. "Automated medical diagnosis of COVID-19 through EfficientNet convolutional neural network." *Applied soft computing* 96 (2020): 106691. https://doi.org/10.1016/j.asoc.2020.106691
[21] Ab Wahab, Mohd Nadhir, Amril Nazir, Anthony Tan Zhen Ren, Mohd Halim Mohd Noor, Muhammad Firdaus Akbar, and Ahmad Sufril Azlan Mohamed. "Efficientnet-lite and hybrid CNN-KNN implementation for facial expression recognition on raspberry pi." *IEEE Access* 9 (2021): 134065-134080. https://doi.org/10.1109/ACCESS.2021.3113337
[22] Tan, Mingxing, and Quoc Le. "Efficientnet: Rethinking model scaling for convolutional neural networks." In *International conference on machine learning*, pp. 6105-6114. PMLR, 2019.
[23] Bishop, Christopher M., and Nasser M. Nasrabadi. "Pattern Recognition and Machine Learning." *Journal of Electronic Imaging* 16, no. 4 (2007): 049901-049901. https://doi.org/10.1117/1.2819119
[24] Lee, Kyuhan, Jinsoo Park, Iljoo Kim, and Youngseok Choi. "Predicting movie success with machine learning techniques: ways to improve accuracy." *Information Systems Frontiers* 20 (2018): 577-588. https://doi.org/10.1007/s10796-016-9689-z
[25] Abd-Ellah, Mahmoud Khaled, Ali Ismail Awad, Ashraf AM Khalaf, and Hesham FA Hamed. "A review on brain tumor diagnosis from MRI images: Practical implications, key achievements, and lessons learned." *Magnetic resonance imaging* 61 (2019): 300-318. https://doi.org/10.1016/j.mri.2019.05.028
[26] Kumar, R. Lokesh, Jagadeesh Kakarla, B. Venkateswarlu Isunuri, and Munesh Singh. "Multi-class brain tumor classification using residual network and global average pooling." *Multimedia Tools and Applications* 80, no. 9 (2021): 13429-13438. https://doi.org/10.1007/s11042-020-10335-4
[27] Hollon, Todd C., Balaji Pandian, Arjun R. Adapa, Esteban Urias, Akshay V. Save, Siri Sahib S. Khalsa, Daniel G. Eichberg et al. "Near real-time intraoperative brain tumor diagnosis using stimulated Raman histology and deep neural networks." *Nature medicine* 26, no. 1 (2020): 52-58. https://doi.org/10.1038/s41591-019-0715-9
[28] Vidiri, Antonello, Andrea Pace, Alessandra Fabi, Marta Maschio, Gaetano Marco Latagliata, Vincenzo Anelli, Francesca Piludu, Carmine Maria Carapella, Giuseppe Giovinazzo, and Simona Marzi. "Early perfusion changes in patients with recurrent high-grade brain tumor treated with Bevacizumab: preliminary results by a quantitative evaluation." *Journal of Experimental & Clinical Cancer Research* 31 (2012): 1-10. https://doi.org/10.1186/1756-9966-31-33
[29] Zhang, Yiqun, Fengju Chen, Lawrence A. Donehower, Michael E. Scheurer, and Chad J. Creighton. "A pediatric brain tumor atlas of genes deregulated by somatic genomic rearrangement." *Nature communications* 12, no. 1 (2021): 937. https://doi.org/10.1038/s41467-021-21081-y
[30] David, Laurianne, Amol Thakkar, Rocío Mercado, and Ola Engkvist. "Molecular representations in AI-driven drug discovery: a review and practical guide." *Journal of Cheminformatics* 12, no. 1 (2020): 56. https://doi.org/10.1186/s13321-020-00460-5
[31] Hammer, Marilyn J. "Ethical considerations for data collection using surveys." *Number 2/March 2017* 44, no. 2 (2017): 157-159.

[32] Lilhore, Umesh Kumar, M. Poongodi, Amandeep Kaur, Sarita Simaiya, Abeer D. Algarni, Hela Elmannai, V. Vijayakumar, Godwin Brown Tunze, and Mounir Hamdi. "Hybrid model for detection of cervical cancer using causal analysis and machine learning techniques." *Computational and Mathematical Methods in Medicine* 2022 (2022). https://doi.org/10.1155/2022/4688327

[33] Ramesh, T. R., Umesh Kumar Lilhore, M. Poongodi, Sarita Simaiya, Amandeep Kaur, and Mounir Hamdi. "Predictive analysis of heart diseases with machine learning approaches." *Malaysian Journal of Computer Science* (2022): 132-148. https://doi.org/10.22452/mjcs.sp2022no1.10

[34] Annam, Sangeetha, and Anshu Singla. "Hyperspectral Image Classification Using Deep Learning Model." *ECS Transactions* 107, no. 1 (2022): 6427. https://doi.org/10.1149/10701.6427ecst

[35] Sood, Deepika, and Anshu Singla. "A Survey of Segmentation Techniques for Medical Images." In *2022 10th International Conference on Reliability, Infocom Technologies and Optimization (Trends and Future Directions)(ICRITO)*, pp. 1-8. IEEE, 2022. https://doi.org/10.1109/ICRITO56286.2022.9964616